Strong biexcitonic effects and exciton-exciton correlations in ZnO

K. Hazu,* T. Sota,† and K. Suzuki
Department of Electrical, Electronics, and Computer Engineering, Waseda University, Shinjuku, Tokyo 169-8555, Japan

S. Adachi‡
Department of Applied Physics, Hokkaido University, Kitaku, Sapporo 060-8628, Japan

SF. Chichibu§
Institute of Applied Physics and Graduate School of Pure and Applied Sciences, University of Tsukuba, 1-1-1 Tennodai, Tsukuba, Ibaraki 305-8573, Japan

G. Cantwell and D. B. Eason
Eagle-Picher Technologies, LLC., 200B. J. Tunnel Blvd., Miami, Oklahoma 74354, USA

D. C. Reynolds and C. W. Litton
Materials and Manufacturing Directorate, Air Force Research Laboratory, Wright-Patterson Air Force Base, Ohio 45433, USA
(Received 12 March 2003; published 30 July 2003)

We have studied experimentally biexcitonic states of ZnO of rather high quality in the low exciton density limit by means of time-integrated and spectrally-resolved four-wave mixing (FWM). FWM emission signals due to biexcitons consisting of two A-hole excitons (AA biexcitons), an A-hole and a B-hole exciton (AB biexcitons), and two B-hole excitons (BB biexcitons) have been clearly observed according to polarization selection rules. The obtained binding energies for AA, AB, and BB biexcitons are 15.6, 16.6, and 4.7 meV, respectively. A brief discussion is also given on the contribution of biexciton and two-pair continuum resonances to the FWM signal.

DOI: 10.1103/PhysRevB.68.033205 PACS number(s): 71.35.Cc, 42.50.Md, 42.62.Fi, 71.55.Eq

Zinc oxide (ZnO) is one of promising materials for light emitting diodes, photodetectors, laser diodes in the blue to ultraviolet wavelength region, transparent field effect transistors, and so on. Recent progress in epitaxial growth technique has again attracted a great deal of researchers to a study of ZnO. A precise knowledge of the bulk material is indispensable to evaluate epitaxially grown crystals.

ZnO crystallizes in the wurtzite structure. Thus the degeneracy of valence bands at Γ-point is lift up due to the crystal field and spin-orbit splitting. The valence bands are usually referred to as A, B, and C valence bands. Therefore, excitons formed in ZnO are called A, B, and C excitons in the lowest order approximation. Excitonic structures in ZnO have been extensively studied,[1–8] and the binding energies are known to be very large due to the small dielectric constant and the large effective masses. With respect to excitonic molecules, the observation of biexciton levels and the determination of their binding energy have usually been carried out using photoluminescence (PL) spectroscopy under intense laser excitation and at low temperature.[9–11] A precise determination of the biexciton levels from PL experiments is, however, very difficult in ZnO due to the large number of final states for biexciton decay within the band of A- and B-excitonic polaritons. The most reliable data on the biexcitonic levels reported so far have been given by Hvam *et al.*[12] using two-photon reabsorption[13,14] and two-photon Raman scattering spectroscopy.[15] However a whole set of biexciton binding energies in the material is not still known and, furthermore, the previous data[12] have not been confirmed by the alternative experimental technique.

Four-wave mixing (FWM) signals due to the biexciton formation associated with two-photon coherence (TPC) are known to be sensitive to the incident polarization,[16,17] and thus the FWM technique is a powerful tool to study the biexciton levels in the low exciton density limit.[18–20] In this paper we report on FWM signals due to biexcitons in the A- and B-exciton systems of ZnO, i.e., biexcitons consisting of two A-hole excitons (AA biexciton, XX_{AA}), one A-hole exciton, and one B-hole exciton (AB biexciton, XX_{AB}), and two B-hole excitons (BB biexciton, XX_{BB}). New sets of eigenenergy and binding energy for biexcitons have been obtained. We have also discussed the dephasing dynamics.

A sample studied herein was a *c*-face bulk ZnO grown by the seeded vapor transport method. Polarized reflectance and photoreflectance spectra of the sample have been published elsewhere.[8] A frequency-doubled, mode-locked Ti:sapphire laser was used as an excitation source in FWM experiments. The fundamental laser produced pulses of 80 fs at a repetition rate of 80 MHz. The frequency-doubled output was divided into two beams with an equal intensity. These pulses with wave vectors $\boldsymbol{k}_1$ and $\boldsymbol{k}_2$, respectively, were superimposed on the sample surface at angle of 6°. The FWM was performed in the $2\boldsymbol{k}_2-\boldsymbol{k}_1$ backward geometry using a degenerate two-pulse configuration. The delay time τ_{12} between two incident pulses was defined to be positive when the $\boldsymbol{k}_1$ pulse precedes the $\boldsymbol{k}_2$ pulse. FWM signals were detected, time integrated, and spectrally resolved, by a combination of a 0.35-m focal length monochromator with a 2400-grooves/mm grating and a multichannel CCD detector. The spectral resolution of the system was about 0.45 meV. Ac-

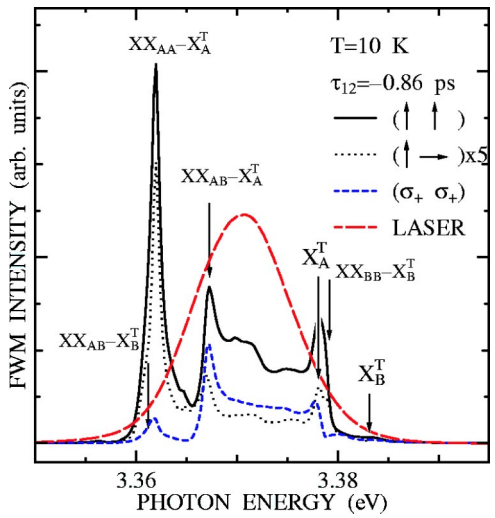

FIG. 1. FWM spectra for $(\uparrow\uparrow)$, $(\uparrow\rightarrow)$, and $(\sigma_+\sigma_+)$ polarizations at a delay time of $\tau_{12}=-0.86$ ps. The laser spectrum is also shown.

cording to circumstances, signals were recorded by a pin photodiode with a phase-sensitive detection method. The excited exciton density was of the order of 10^{16} cm^{-3}, which was far below the Mott density ($\approx 5\times 10^{18}$ cm^{-3}). Throughout the measurements, the sample was held in a closed-cycle helium cryostat and its temperature was maintained to be $T=10$ K. All data reported herein were measured from the (0001) surface.

It is known that for negative delay times the signal is entirely due to Coulomb-induced nonlinearities.[21] In this case the $\boldsymbol{k}_2$ pulse arrives first, which contributes in second order to the signal. The delay-time dynamics is thus given by TPCs produced by the $\boldsymbol{k}_2$ pulse in the system and thus is closely related to biexciton and two-pair continuum resonances created by the two-photon absorption. According to the polarization selection rules, while the formation of XX_{AA} and XX_{BB} is allowed for $(\uparrow\uparrow)$ and $(\uparrow\rightarrow)$ polarizations alone,[22] the formation of XX_{AB} is allowed for all the three polarizations.[17]

Figure 1 shows typical FWM spectra at $\tau_{12}=-0.86$ ps for $(\uparrow\uparrow)$, $(\uparrow\rightarrow)$, and $(\sigma_+\sigma_+)$ polarizations, where the laser spectrum is also shown. To study biexcitons, the off-resonance excitation was used as in Ref. 16. The arrows labeled X_A^T and X_B^T indicate the transverse exciton resonance energies assigned experimentally. As for the notation, for example, $X_{A(B)}^{T(L)}$ denotes the transverse (T) [longitudinal (L)] A (B) exciton. The emission signals labeled $XX_{AB}-X_A^T$ and $XX_{AB}-X_B^T$ appear for all the three polarizations and may be assigned as the signal induced by the transition between XX_{AB} and X_A and between XX_{AB} and X_B, respectively. Note the emission signal labeled $XX_{AB}-X_B^T$ appears at lower energy side of the emission labeled $XX_{AA}-X_A^T$. The $XX_{AA}-X_A^T$ emission is pronounced for $(\uparrow\uparrow)$ and $(\uparrow\rightarrow)$ polarizations and, thus, is assigned as the emission due to XX_{AA}. The emission labeled $XX_{BB}-X_B^T$ appears only for $(\uparrow\uparrow)$ and $(\uparrow\rightarrow)$ polarizations, and is assigned as the emission due to XX_{BB}.

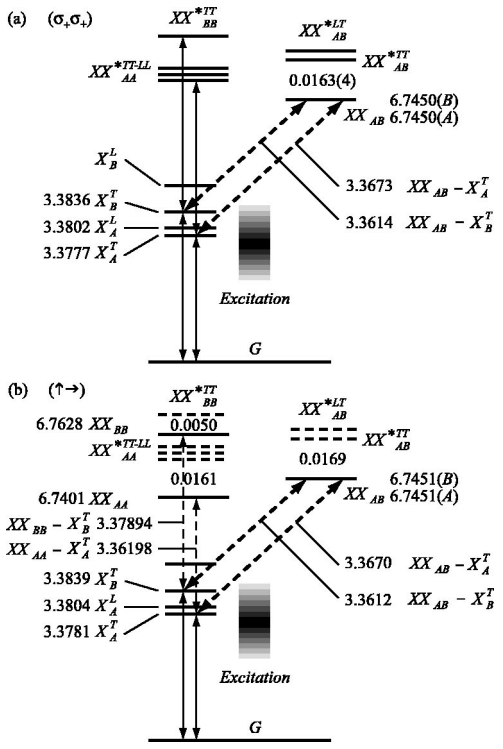

FIG. 2. Possible transition schemes for the exciton-biexciton system under the present excitation condition for (a) $(\sigma_+\sigma_+)$ and (b) $(\uparrow\rightarrow)$ polarizations, which are obtained from Fig. 1. The dashed levels in Fig. 2 (b) indicate that they are inactive in generating FWM signals.

We have obtained the emission peak energies of our interest by fitting Gaussian line shape functions to the obtained spectra. With respect to the resonance energy of X_B^T, we have used spectrally resolved FWM spectra at $\tau_{12}>0$, which are not shown herein. Figures 2(a) and 2(b) show optical transitions among the energy levels obtained from Fig. 1 for $(\sigma_+\sigma_+)$ and $(\uparrow\rightarrow)$ polarizations, respectively, where $XX^{*\gamma\delta}_{\alpha\beta}$ denotes two-pair continuum states consisting of two excitons X_α^γ and X_β^δ. Here the excitation laser bandwidth is also schematically shown. In Fig. 2(b) the dashed levels mean that the transitions via them are inactive in signal generation for $(\uparrow\rightarrow)$ polarization. The obtained eigenenergies for each biexciton and the corresponding binding energy are tabulated in Table I, where the most reliable previous

TABLE I. Eigenenergies (in units of eV) and binding energies (in units of meV) for the AA, AB, and BB biexcitons of ZnO.

Reference	E_{AA}	E_{AB}	E_{BB}
Hvam *et al.*[a]	6.7355 ± 0.0010	6.7407 ± 0.0006	6.7469 ± 0.0008
Present result[b]	6.7396 ± 0.0005	6.7446 ± 0.0005	6.7622 ± 0.0006
	E_{AA}^b	E_{AB}^b	E_{BB}^b
Hvam *et al.*[a]	14.7	9.5	3.3
Present result[b]	15.6 ± 0.5	16.6 ± 0.3	4.7 ± 0.3

[a]Reference 12.

[b]With respect to the present results of the eigenenergy and the binding energy, see the text.

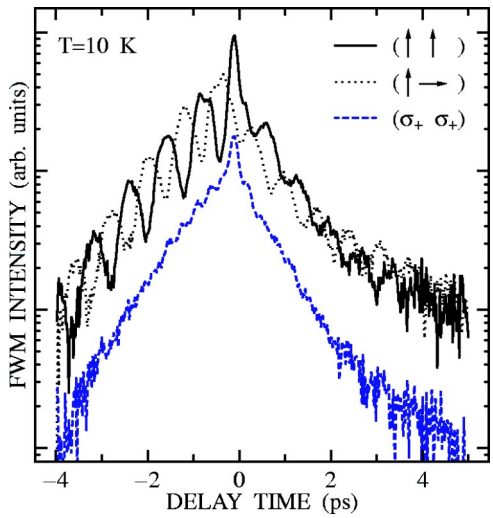

FIG. 3. FWM traces as a function of delay time τ_{12} for $(\uparrow\uparrow)$, $(\uparrow\rightarrow)$, and $(\sigma_+\sigma_+)$ polarizations. The FWM trace for $(\sigma_+\sigma_+)$ polarization is scaled by a factor of 0.3.

results[12] are also shown. Here E_{AA} (E^b_{AA}), E_{AB} (E^b_{AB}), and E_{BB} (E^b_{BB}) denote, respectively, the eigenenergy (binding energy) for XX_{AA}, XX_{AB}, and XX_{BB}. Eigenenergies, binding energies, and error bars for the present work have been determined from the analysis of a series of data including Fig. 1, which were measured varying the excitation laser wavelength. Therefore the numbers in Table I and those shown in Fig. 2 do not show a one-to-one correspondence. Note that all the binding energies in the previous paper[12] are measured from the lowest free exciton state $E_{A\Gamma_{1,2}}=3.3751$ eV.[23]

In the following we confirm our assignment summarized in Fig. 2 and Table I. Relative ratios of the integrated signal intensity induced by biexcitons have been found to be almost the same for the $(\uparrow\rightarrow)$ polarization. Here, taking into account that the signal intensity due to biexcitons depends on the excitation wavelength, we have used Fig. 1 and other data (not shown), which were measured at the slightly shorter wavelength than that in Fig. 1. The intensity ratio can be estimated by comparing the product of the oscillator strength appearing in the third-order nonlinear response.[16] If we assume that the relative oscillator strength between A- and B-hole related transitions is given by the valence-band function to $|\mu_A|^2/|\mu_B|^2\approx|\nu_A|^2/|\nu_B|^2\approx|\nu_{A,AB}|^2/|\nu_{B,AB}|^2\approx 1$,[24,25] the intensity ratio is approximately given by $I_{XX_{AA}}:I_{XX_{AB}}:I_{XX_{BB}}\approx 1:1:1$. Here μ_α, ν_α, and $\nu_{\alpha,AB}$ $(\alpha=A,B)$ represent the dipole matrix elements of the transitions $X_\alpha-G$, $XX_{\alpha\alpha}-X_\alpha$, and $XX_{AB}-X_\alpha$, respectively. A good agreement between the calculated and the experimental ratios are obtained. Therefore, we believe that the aforementioned assignment is plausible.

The observed large binding energies of biexcitons enable us to study the influence of the biexciton binding on the scattering process of the involved excitons. Figure 3 shows time-integrated FWM traces as a function of τ_{12}, which were recorded using a pin photodiode under the same excitation condition shown in Fig. 1. Overall features of the FWM traces are as follows. The intensity of the FWM signal is almost the same for all three polarizations, and the relative intensity is longer for $\tau_{12}<0$ than for $\tau_{12}>0$. The high-contrast beating is observed only for $(\uparrow\rightarrow)$, and $(\uparrow\uparrow)$ polarizations, and both their phases change by π, to suggest that the origin of the beating is the quantum interference. We demonstrate below that the FWM traces in the time domain are well explained by the transition scheme shown in Fig. 2 within the third-order nonlinearity response. Note that the signal at $\tau_{12}<0$ is generated dominantly by TPCs.[21]

For $(\uparrow\rightarrow)$ polarization, the signal is generated only via X^γ_α and $XX_{\alpha\beta}$ $(\alpha,\beta=A,B$ and $\gamma=T,L)$ resonances for both $\tau_{12}<0$ and $\tau_{12}>0$ as shown in Fig. 2(b).[21,26–28] Therefore $XX_{\alpha\beta}$ TPCs dominate the signal generation processes. The observed beating period of 0.79 ps for $\tau_{12}<0$ is converted to an energy separation of 5.2 meV. Its origin can be assigned as the quantum interference between the $XX_{AA}-X^T_A$ and $XX_{AB}-X^T_A$ transitions with an energy separation of 5.1 meV, as shown in Fig. 2(b). For $\tau_{12}>0$, Fig. 3 shows that the decay process of the signal consists of two components with the same beating period. The period is observed to be 0.70 ps, which corresponds to the energy separation of 5.9 meV. The energy difference in the X^T_A and X^T_B resonances is 5.8 meV. Thus, the observed beating originates from the $X^T_A-G-X^T_B$ system and the $X^T_A-XX_{AB}-X^T_B$ system. It is known that FWM signals generated by four-particle correlations in biexciton and two-pair continuum states are dominant signals. Therefore the initial large FWM signal is attributed to the signal generated in the latter system and the second small FWM signal with the longer decay time is attributed to the signal generated in the former system.

For the $(\sigma_+\sigma_+)$ polarization, the relatively large signal at $\tau_{12}\approx 0$ observed in Fig. 3 reflects the presence of contributions from the $XX^{*\gamma\delta}_{\alpha\beta}$ resonances,[29] and the formation of $XX_{\alpha\alpha}$ is inhibited because $XX_{\alpha\alpha}$ consists of excitons with different spins. Thus the signal is generated via X^γ_α, XX_{AB}, and $XX^{*\gamma\delta}_{\alpha\beta}$ resonances, as shown in Fig. 2(a). The lack of the XX_{AA} state leads to the disappearance of the pronounced beating observed for the $(\uparrow\rightarrow)$ polarization and $\tau_{12}<0$. For $\tau_{12}>0$, the $X^T_A-X^T_B$ beating is not observed in the initial decay signal. This means that there exist mechanisms which produce a beating with the same period but with the phase shifted by π to wash out the $X^T_A-X^T_B$ beating due to the $X^T_A-XX_{AB}-X^T_B$ system. Recognizing that the formation of XX_{AB} suppresses the contribution of $XX^{*\gamma\delta}_{AB}$ to the signal generation processes, it follows from Fig. 2(a) that the possible origin of such beating is attributed to a pair of two-level systems consisting of the $XX^{*TT}_{AA}-X^T_A$ and $XX^{*TT}_{BB}-X^T_B$ transitions. The low-contrast beating with a period of 0.31 ps is observed for both $\tau_{12}<0$ and $\tau_{12}>0$. Its origin may be attributed to the polarization interference between the $XX_{AB}-X^T_A$ and $XX^{*LT}_{AA}-X^L_A$ transitions and/or the quantum interference in the $XX_{AB}-X^T_A-XX^{*TL}_{AA}$ three-level system, all of which produce the beating period of 0.32 ps.

For $(\uparrow\uparrow)$ polarization, the formation of biexcitons XX_{AA} and XX_{BB} is allowed. Thus the beating with a period of 0.79 ps, observed for $\tau_{12}<0$, is assigned as the quantum interfer-

ence in the $XX_{AB}-X_A^T-XX_{AA}$ three-level system in the same way for $(\uparrow\rightarrow)$ polarization. The beating observed for $\tau_{12}>0$ is the $X_A^T-X_B^T$ beating because the energy separation estimated from the beating period coincides with that between the X_A^T and X_B^T resonances. The survival of the $X_A^T-X_B^T$ beating for the $(\uparrow\uparrow)$ polarization is explained by recognizing that the formation of biexcitons suppresses contributions from both the XX_{AA}^{*TT} and XX_{BB}^{*TT} states to the signal generation processes. It follows that the contribution of the $XX_{\alpha\beta}^{*\gamma\delta}$ states is the largest for the $(\sigma_+\sigma_+)$ polarization and almost vanishes for the $(\uparrow\rightarrow)$ polarization. This is consistent with the order of the initial signal decay time observed in Fig. 3, i.e., 0.75, 1.10, and 0.83 ps for $(\sigma_+\sigma_+)$, $(\uparrow\rightarrow)$, and $(\uparrow\uparrow)$ polarizations. Therefore our explanation is self-consistent, to demonstrate clearly that the formation of $XX_{\alpha\beta}$ suppresses the scattering events of involved excitons.

With respect to the $X_A^T-X_B^T$ beating for $\tau_{12}>0$, the following is expected based on the above discussion. When the excitation wavelength is shortened so that the biexciton states stop functioning properly, the $X_A^T-X_B^T$ beating appears for both $(\uparrow\uparrow)$ and $(\sigma_+\sigma_+)$ polarizations but disappears for the $(\uparrow\rightarrow)$ polarization. Simultaneously, the initial decay time becomes faster because of the destructive interference caused by the $XX_{\alpha\beta}^{*\gamma\delta}$ states. Preliminary experiments suggest that this is the case. The result will be published elsewhere.

In summary, we have experimentally studied FWM signals in ZnO and discussed the dephasing properties of the exciton-biexciton system within the third-order nonlinearity response in the low exciton density limit. The signals due to AA, AB, and BB biexcitons have been clearly observed according to the polarization selection rules and the following binding energies have been obtained: $E_{AA}^b=15.6\pm0.5$ meV for the AA biexciton, $E_{AB}^b=16.6\pm0.3$ meV for the AB biexciton, and $E_{BB}^b=4.7\pm0.3$ meV for the BB biexciton. We believe that the results obtained herein are the most plausible at present in the low exciton density limit.

*Electronic address: kouji@moegi.waseda.jp
†Electronic address: tkyksota@waseda.jp
‡Also at CREST, Japan Science and Technology Corporation.
§Also at NICP, ERATO, Japan Science and Technology Corporation (JST) and Photodynamics Research Center, RIKEN (Institute of Physical and Chemical Research).

[1] D.G. Thomas, J. Phys. Chem. Solids **15**, 86 (1960).
[2] J.J. Hopfield, J. Phys. Chem. Solids **15**, 97 (1960).
[3] Y.S. Park, C.W. Litton, T.C. Collins, and D.C. Reynolds, Phys. Rev. **143**, 512 (1966).
[4] K. Hümmer and P. Gebhardt, Phys. Status Solidi B **85**, 271 (1978).
[5] J. Lagois, Phys. Rev. B **23**, 5511 (1981).
[6] D.C. Reynolds, D.C. Look, B. Jogai, C.W. Litton, G. Cantwell, and W.C. Harsch, Phys. Rev. B **60**, 2340 (1999).
[7] D.C. Reynolds, D.C. Look, B. Jogai, and T.C. Collins, Appl. Phys. Lett. **79**, 3794 (2001).
[8] SF. Chichibu, T. Sota, G. Cantwell, D.B. Eason, and C.W. Litton, J. Appl. Phys. **93**, 756 (2003).
[9] J.H. Hvam, Phys. Status Solidi B **63**, 511 (1974).
[10] Y. Segawa and S. Namba, Solid State Commun. **17**, 489 (1975).
[11] S. Miyamoto and S. Shionoya, J. Lumin. **12/13**, 563 (1976).
[12] J.M. Hvam, G. Blattner, M. Reuscher, and C. Klingshirn, Phys. Status Solidi B **118**, 179 (1983).
[13] H. Schrey and C. Klingshirn, Phys. Status Solidi B **93**, 679 (1979).
[14] J.M. Hvam, Phys. Status Solidi B **93**, 581 (1979).
[15] H. Schrey and C. Klingshirn, Solid State Commun. **28**, 9 (1979).
[16] H.P. Wagner, W. Langbein, and J.M. Hvam, Phys. Rev. B **59**, 4584 (1999).
[17] S. Adachi, S. Muto, K. Hazu, T. Sota, K. Suzuki, SF. Chichibu, and T. Mukai, Phys. Rev. B **67**, 205212 (2003).
[18] B.F. Feuerbacher, J. Kuhl, and K. Ploog, Phys. Rev. B **43**, 2439 (1991).
[19] D.J. Lovering, R.T. Phillips, G.J. Denton, and G.W. Smith, Phys. Rev. Lett. **68**, 1880 (1992).
[20] H. Wang, J. Shah, T.C. Damen, and L.N. Pfeiffer, Solid State Commun. **91**, 869 (1994).
[21] W. Langbein, T. Meire, S.W. Koch, and J.M. Hvam, J. Opt. Soc. Am. B **18**, 1318 (2001).
[22] P. Kner, W. Schäfer, R. Lövenich, and D.S. Chemla, Phys. Rev. Lett. **81**, 5386 (1998).
[23] G. Blattner, G. Kurtze, G. Schmieder, and C. Klingshim, Phys. Rev. B **25**, 7413 (1982).
[24] K. Hazu, K. Torii, T. Sota, K. Suzuki, S. Adachi, SF. Chichibu, C. W. Litton, and D. B. Eason (unpublished).
[25] K. Torii, T. Sota, and SF. Chichibu (unpublished).
[26] For example, see, V.M. Axt, B. Haase, and U. Neukirch, Phys. Rev. Lett. **86**, 4620 (2001), and references cited therein.
[27] For example, see, K. Siantidis, V.M. Axt, and T. Kuhn, Phys. Rev. B **65**, 035303 (2001), and references cited therein.
[28] W. Langbein, and J.M. Hvam, Phys. Rev. B **61**, 1692 (2000); Phys. Status Solidi A **190**, 167 (2002).
[29] D. Birkedal, V.G. Lyssenko, J.M. Hvam, and K. El Sayed, Phys. Rev. B **54**, 14 250 (1996).